Journal of American Science

Websites:
http://www.jofamericanscience.org
http://www.sciencepub.net

Emails:
editor@sciencepub.net
sciencepub@gmail.com

MARSLAND PRESS
Multidisciplinary Academic Journal Publisher

Electrostatic Analysis of a Smart Piezoceramic Plate by using Exact Solution and Finite Element Method for Two Electrical Boundary Conditions of SC and OC

Alireza Pouladkhan

Department of Civil Engineering, The University of British Columbia, Vancouver, BC, Canada
a.pouladkhan@alumni.ubc.ca

Abstract: This paper presents an exact solution and a finite element method (FEM) for a Piezoceramic Plate under static load. The rectangular plate is made from polarized ceramics (piezoceramic). The unbounded ceramic plate is poled in the thickness direction. The major surfaces of the plate are under a normal traction and are electroded. Two cases of shorted and open electrodes (short circuit and open circuit) will be considered. The traction-produced charge or voltage on the electrodes can be used to detect the pressure electrically. Finally, a finite element model will be used to compare the results with an exact solution. The study uses *ABAQUS* (*v.6.7*) software to derive the finite element model of the ceramic plate.
[Pouladkhan A. **Electrostatic Analysis of a Smart Piezoceramic Plate by using Exact Solution and Finite Element Method for Two Electrical Boundary Conditions of SC and OC.** *J Am Sci* 2021;17(4):1-8]. ISSN 1545-1003 (print); ISSN 2375-7264 (online). http://www.jofamericanscience.org. 1. doi:10.7537/marsjas170421.01.

Keywords: Finite element method; Unbounded ceramic plate; Normal traction; Short circuit; Open circuit

1. Introduction

The pattern and relationships between species diversity and Piezoelectric materials are used widely in transducers such as ultrasonic transmitters and receivers, sonar for underwater applications, and as actuators for precision positioning devices. Piezoelectric materials exhibit Electromechanical Coupling, which is useful for the design of devices for sensing and actuation. The coupling is exhibited in the fact that piezoelectric materials produce an electrical displacement when a mechanical stress is applied and can produce mechanical strain under the application of an electric field. Due to the fact that the mechanical-to-electrical coupling was discovered first, this property is termed the direct piezoelectric effect, while the electrical-to-mechanical coupling is termed the converse piezoelectric effect [1].

The physical basis for piezoelectricity in solids is widely studied by physicists and materials scientists. Most piezoelectric materials belong to a class of crystalline solids. Crystals are solids in which the atoms are arranged in a single pattern repeated throughout the body. Crystalline materials are highly ordered, and an understanding of the bulk properties of the material can begin by understanding the properties of the crystals repeated throughout the solid. The individual crystals in a solid can be thought of as building blocks for the material. Joining crystals together produces a three-dimensional arrangement of the crystals called a unit cell.

One of the most important properties of a unit cell in relation to piezoelectricity is the polarity of the unit cell structure. Crystallographers have studied the structure of unit cells and classified them into a set of 32 crystal classes or point groups. Each point group is characterized by a particular arrangement of the constituent atoms. Of these 32-point groups, 10 have been shown to exhibit a polar axis in which there is a net separation between positive charges in the crystal and their associated negative charges. This separation of charge produces an electric dipole, which can give rise to piezoelectricity [1,2].

Induced strain actuators like piezoelectric materials have been effectively used as integrated sensors and actuators for monitoring and further controlling the mechanical behavior of advanced structures [3,4]. Over the past decade, Finite Element Analysis (FEA) techniques have been employed to model the overall structural response involving the electromechanical coupling effects of the piezoelectric sensing/actuating elements [5]. Superior to analytical methods, the FEA technique provides greater geometric flexibility and allows use of more complex electrical and mechanical boundary conditions. Although much research effort has been devoted to finite element formulation for the electromechanical coupling effects of piezoelectric materials (Tzou and Tseng, 1990; Ha et al., 1991), fully electromechanical-coupled piezoelectric elements have just recently become available in commercial FEA software [6].

Before the new piezoelectric capability was developed in commercial FEA codes, the induced strain actuation function of piezoelectric materials had been modeled using analogous thermal expansion/contraction characteristics of structural materials [7]. This method was helpful in the studies

of the resulting stress distribution in actuators and host substructures and the overall deformation of integrated structures under static actuation. However, the intrinsic electromechanical coupling effects of piezoelectric materials cannot be modeled. Moreover, the dynamic actuation response of piezoelectric actuators on host substructures is difficult to implement by this method.

The new piezoelectric finite element capability in commercial FEA packages such as ABAQUS gives convenient access to perform both static and dynamic analysis for the fully coupled piezoelectric and structural response. In addition, since most commercialized FEA packages are generally equipped with well-developed pre and post-processors and user-friendly interactive graphics working environments, the time-consuming tasks of finite element model generation and solution extraction can be significantly reduced [7]. A finite element model for a sandwich plate containing a piezoelectric core for deflection and stress analysis using ABAQUS software were investigated by Pouladkhan et al. [8]. Pouladkhan et al. [9] presented an exact solution and a finite element method (using ABAQUS software) for a smart piezoelectric ceramic rod under static load.

2. Linear Piezoelectricity for Infinitesimal Fields

Nonlinear theory of Electroelasticity is used for large deformations and strong electric fields. In linear theory like Piezoelectricity, we can specialize the nonlinear equations to the case of infinitesimal deformations and fields, which results in the linear theory of piezoelectricity. For Linearization, we reduce the nonlinear electroelastic equations in the nonlinear theory to the linear theory of piezoelectricity for infinitesimal deformations and fields. We consider small amplitude motions of an electroelastic body around its reference state due to small mechanical and electrical loads [10]. It is assumed that the displacement gradient is infinitesimal in the following sense that:

$$\|u_{i,K}\| \ll 1 \tag{1}$$

Under some norm, e.g., $\|u_{i,K}\| = max|u_{i,K}|$. It is also assumed that the electric potential gradient $\phi_{,K}$ is infinitesimal.

$$\|\phi_{,K}\| \ll 1 \tag{2}$$

We neglect powers of $u_{i,K}$ and $\phi_{,K}$ higher than the first as well as their products in all expressions. The linear terms themselves are also dropped in comparison with any finite quantity such the Kronecker delta or 1. Under (1),

$$\begin{aligned}\frac{\partial u_i}{\partial X_K} &= \frac{\partial u_i}{\partial y_k} y_{k,K} = \frac{\partial u_i}{\partial y_k}(\delta_{kK} + u_{k,K}) \\ &\cong \frac{\partial u_i}{\partial y_k}\delta_{kK} \\ \phi_{,K} &= \phi_{,i} y_{i,K} \cong \phi_{,i}\delta_{iK}\end{aligned} \tag{3}$$

Which implies that, to the first order of approximation, the displacement and potential gradients calculated from the material and spatial coordinates are numerically equal. Therefore, within the linear theory, there is no need to distinguish capital and lowercase indices. Only lowercase indices will be used in the linear theory. The material time derivative of an infinitesimal field variable $f(y,t)$ is simply the partial derivative with respect to t:

$$\begin{aligned}\frac{Df}{Dt} &= \frac{\partial f}{\partial t}|_{X\ fixed} \\ &= \frac{\partial f}{\partial t}|_{y\ fixed} + \frac{\partial f}{\partial y_i}|_{t\ fixed}\frac{\partial y_i}{\partial t}|_{X\ fixed} \\ &= \frac{\partial f}{\partial t}|_{y\ fixed} + v_i\frac{\partial f}{\partial y_i} \cong \frac{\partial f}{\partial t}|_{y\ fixed}\end{aligned} \tag{4}$$

For the finite strain tensor:

$$\begin{aligned}S_{KL} &= \frac{1}{2}(u_{L,K} + u_{K,L} + u_{M,K}u_{M,L}) \\ &\cong \frac{1}{2}(u_{L,K} + u_{K,L})\end{aligned} \tag{5}$$

In the linear theory, the infinitesimal strain tensor will be denoted by:

$$S_{kl} = \frac{1}{2}(u_{l,k} + u_{k,l}) \tag{6}$$

The material electric field becomes:

$$E_K = E_i y_{i,K} \cong E_i\delta_{iK} \to E_k \tag{7}$$

Similarly,

$$\begin{aligned}&\sigma_{ij}^E \cong 0\ ,\sigma_{ij}^M \cong 0\ ,\sigma_{ij} \cong \sigma_{ij}^S \cong \tau_{ij} \\ &M_{Lj} \cong 0\ ,K_{Lj} \cong F_{Lj} \cong \delta_{Ki}\sigma_{ij}\ ,T_{KL}^S \\ &\qquad \cong \delta_{Ki}\delta_{Lj}\sigma_{ij} \\ &\mathcal{P}_K \to P_k\ ,\mathcal{D}_K \to D_k\end{aligned} \tag{8}$$

Where:

σ_{ij}^E = Electrostatic strees tensor

σ_{ij}^M , M_{Lj} = Symmetric Maxwell stress tensor in spatial, two point

σ_{ij} = Cauchy stress tensor

σ_{ij}^S , F_{Lj} , T_{KL}^S = Symmetric stress tensor in spatial, two point, and material form

τ_{ij} , K_{Lj} = Total stress tensor in spatial, two point

$\mathcal{P}_K$ = Reference electric polarization vector

$\mathcal{D}_K$ = Reference electric displacement vector

Since the various stress tensors are either approximately zero (quadratic in the infinitesimal gradients) or about the same, we will use T_{ij} to denote the stress tensor that is linear in the infinitesimal gradients. This is according to the IEEE Standard on Piezoelectricity. The notation for the rest of the linear theory will also follow the IEEE Standard [11]. Then:

$$\begin{aligned}&\sigma_{ij} \cong \sigma_{ij}^S \cong \tau_{ij} \to T_{ij}\\ &K_{Lj} \cong F_{Lj} \cong \delta_{Li}\sigma_{ij} \to T_{ij}\\ &T_{KL}^S \cong \delta_{Ki}\delta_{Lj}\sigma_{ij} \to T_{kl}\end{aligned} \tag{9}$$

For small fields the total free energy can be approximated by:

$$\begin{aligned}\rho_0\hat{\psi}(S_{KL}, E_K) &= \rho_0\psi(S_{KL}, E_K)\\ &\quad -\frac{1}{2}\varepsilon_0 J E_K E_K\\ &\cong \frac{1}{2}c_{2\,ABCD}S_{AB}S_{CD} - e_{ABC}E_A S_{BC}\\ &\quad -\frac{1}{2}\chi_{2\,AB}E_A E_B\\ &\quad -\frac{1}{2}\varepsilon_0 J E_K E_K\\ &\to \frac{1}{2}c_{ijkl}^E S_{ij}S_{kl} - e_{ijk}E_i S_{jk} - \frac{1}{2}\varepsilon_{ij}^S E_i E_j\\ &\quad = H(S_{kl}, E_k)\end{aligned} \tag{10}$$

Where:

$$\varepsilon_{ij}^S = \chi_{2\,ij} + \varepsilon_0\delta_{ij} \tag{11}$$

The superscript E in c_{ijkl}^E indicates that the independent electric constitutive variable is the electric field $\boldsymbol{E}$. The superscript S in ε_{ij}^S indicates that the mechanical constitutive variable is the strain tensor $\boldsymbol{S}$. We have also denoted the total free energy of the linear theory by H, which is usually called the electric enthalpy. The electrical enthalpy (H) in a piezoelectric body is an energy quantity similar to strain energy in an elastic structure. The constitutive relations generated by H are:

$$\begin{aligned}T_{ij} &= \frac{\partial H}{\partial S_{ij}} = c_{ijkl}^E S_{kl} - e_{kij}E_k\\ D_i &= -\frac{\partial H}{\partial E_i} = e_{ikl}S_{kl} + \varepsilon_{ik}^S E_k\end{aligned} \tag{12}$$

Where:

c_{ijkl}^E = Elastic stiffness constants
e_{kij} = Piezoelectric stress constants
ε_{ik} = Dielectric constants

Hence **T**, **D** and **P** are also infinitesimal. The material constants in Equation (12) have the following symmetries:

$$\begin{aligned}&c_{ijkl}^E = c_{jikl}^E = c_{klij}^E\\ &e_{kij} = e_{kji}\\ &\varepsilon_{ij}^S = \varepsilon_{ji}^S\end{aligned} \tag{13}$$

We also assume that the *elastic* and *dielectric material tensors* are positive definite in the following sense:

$$\begin{aligned}&c_{ijkl}^E S_{ij}S_{kl} \geq 0 \; for\; any\; S_{ij}\\ &\qquad\qquad = S_{ji}\\ &and\; c_{ijkl}^E S_{ij}S_{kl} = 0 \to S_{ij}\\ &\qquad\qquad = 0\\ &\varepsilon_{ij}^S E_i E_j \geq 0 \; for\; any\; E_i\\ &and\; \varepsilon_{ij}^S E_i E_j = 0 \to E_i = 0\end{aligned} \tag{14}$$

3. Compact Matrix Notation

We now introduce a compact matrix notation. This notation consists of replacing pairs of indices ij or kl by single indices p or q where i, j, k and l take the values of 1, 2, and 3, and p and q take the values 1, 2, 3, 4, 5, and 6 according to [10]:

$$\begin{array}{l} ij\; or\; kl \\ : 11 \;\; 22 \;\; 33 \;\; 23\; or\; 32 \;\; 31\; or\; 13 \;\; 12\; or\; 21 \\ p\; or\; q: \;\; 1 \;\; 2 \;\; 3 \;\;\;\; 4 \;\;\;\;\;\; 5 \;\;\;\;\;\; 6 \end{array} \tag{15}$$

Thus

$$\begin{aligned}&c_{ijkl} \to c_{pq}\,, e_{ikl} \to e_{ip}\,, T_{ij}\\ &\qquad\qquad \to T_p\end{aligned} \tag{16}$$

For the strain tensor, we introduce S_p such that:

$$\begin{aligned}&S_1 = S_{11}\,,\; S_2 = S_{22}\,,\; S_3\\ &\qquad\qquad = S_{33}\\ &S_4 = 2S_{23}\,,\; S_5 = 2S_{31}\,,\; S_6\\ &\qquad\qquad = 2S_{12}\end{aligned} \tag{17}$$

The constitutive relations in Equation (12) can then be written as:

$$\begin{aligned}T_p &= c_{pq}^E S_q - e_{kp}E_k\\ D_i &= e_{iq}S_q + \varepsilon_{ik}^S E_k\end{aligned} \tag{18}$$

In matrix form, Equation (18) becomes:

$$\begin{Bmatrix} T_1 \\ T_2 \\ T_3 \\ T_4 \\ T_5 \\ T_6 \end{Bmatrix} = \begin{pmatrix} c_{11}^E & c_{12}^E & c_{13}^E & c_{14}^E & c_{15}^E & c_{16}^E \\ c_{21}^E & c_{22}^E & c_{23}^E & c_{24}^E & c_{25}^E & c_{26}^E \\ c_{31}^E & c_{32}^E & c_{33}^E & c_{34}^E & c_{35}^E & c_{36}^E \\ c_{41}^E & c_{42}^E & c_{43}^E & c_{44}^E & c_{45}^E & c_{46}^E \\ c_{51}^E & c_{52}^E & c_{53}^E & c_{54}^E & c_{55}^E & c_{56}^E \\ c_{61}^E & c_{62}^E & c_{63}^E & c_{64}^E & c_{65}^E & c_{66}^E \end{pmatrix} \begin{Bmatrix} S_1 \\ S_2 \\ S_3 \\ S_4 \\ S_5 \\ S_6 \end{Bmatrix} - \begin{pmatrix} e_{11} & e_{21} & e_{31} \\ e_{12} & e_{22} & e_{32} \\ e_{13} & e_{23} & e_{33} \\ e_{14} & e_{24} & e_{34} \\ e_{15} & e_{25} & e_{35} \\ e_{16} & e_{26} & e_{36} \end{pmatrix} \begin{Bmatrix} E_1 \\ E_2 \\ E_3 \end{Bmatrix} \quad (19)$$

$$\begin{Bmatrix} D_1 \\ D_2 \\ D_3 \end{Bmatrix} = \begin{pmatrix} e_{11} & e_{12} & e_{13} & e_{14} & e_{15} & e_{16} \\ e_{21} & e_{22} & e_{23} & e_{24} & e_{25} & e_{26} \\ e_{31} & e_{32} & e_{33} & e_{34} & e_{35} & e_{36} \end{pmatrix} \begin{Bmatrix} S_1 \\ S_2 \\ S_3 \\ S_4 \\ S_5 \\ S_6 \end{Bmatrix} + \begin{pmatrix} \varepsilon_{11}^S & \varepsilon_{12}^S & \varepsilon_{13}^S \\ \varepsilon_{21}^S & \varepsilon_{22}^S & \varepsilon_{23}^S \\ \varepsilon_{31}^S & \varepsilon_{32}^S & \varepsilon_{33}^S \end{pmatrix} \begin{Bmatrix} E_1 \\ E_2 \\ E_3 \end{Bmatrix}$$

4. Displacement – Potential Formulation

In summary, the linear theory of piezoelectricity consists of the *equations* of *motion* and *charge* [10]:

$$T_{ji,j} + \rho f_i = \rho \ddot{u}_i \quad , \quad D_{i,i} = \rho_e \quad (20)$$

Constitutive relations:

$$T_{ij} = c_{ijkl} S_{kl} - e_{kij} E_k \quad , \quad D_i = e_{ijk} S_{jk} + \varepsilon_{ij} E_j \quad (21)$$

And the strain-displacement and electric field-potential relations:

$$S_{ij} = (u_{i,j} + u_{j,i})/2 \quad , \quad E_i = -\phi_{,i} \quad (22)$$

Where **u** is the mechanical displacement vector, **T** is the stress tensor, **S** is the strain tensor, **E** is the electric field, **D** is the electric displacement (electric flux density), ϕ is the electric potential, ρ is the known reference mass density, ρ_e is the body free charge density, and **f** is the body force per unit mass. We have neglected the superscripts in the material constants. With successive substitutions from Equations (21) and (22), Equation (20) can be written as four equations for **u** and:

$$c_{ijkl} u_{k,lj} + e_{kij} \phi_{,kj} + \rho f_i = \rho \ddot{u}_i$$
$$e_{ikl} u_{k,li} - \varepsilon_{ij} \phi_{,ij} = \rho_e \quad (23)$$

5. Thickness Stretch of a Ceramic Plate

Consider an unbounded ceramic plate poled in the thickness direction. The major surfaces of the plate are under a normal traction p and are electroded. Two cases of shorted and open electrodes (short circuit and open circuit) will be considered. The traction-produced charge or voltage on the electrodes can be used to detect the pressure electrically. This problem is an electrostatic case, which is very formal in the piezoelectric problems. Fig. 1 shows an electroded ceramic plate under mechanical loads.

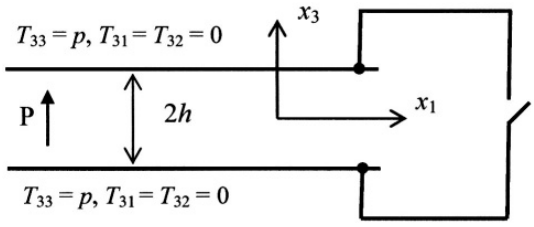

Fig. 1. An electroded ceramic plate under mechanical loads [10].

5.1. Boundary Value Problem

The boundary value problem is:

$$T_{ji,j} = 0 \ , \ D_{i,i} = 0 \ \text{ in } \ V$$
$$T_{ij} = c_{ijkl}^E S_{kl} - e_{kij} E_k \ , \ D_i = e_{ikl} S_{kl} + \varepsilon_{ik}^S E_k \ \text{ in } \ V$$
$$S_{ij} = (u_{i,j} + u_{j,i})/2 \ , \ E_i = -\phi_{,i} \ \text{ in } \ V$$
$$T_{ji} n_j = p \delta_{3i} \ , \ x_3 = \pm h$$
$$\phi(x_3 = h) = \phi(x_3 = -h) \ , \ \text{if the electrodes are shorted}$$
$$D_3(x_3 = \pm h) = 0 \ , \ \text{if the electrodes are open} \quad (24)$$

Consider the possibility of the following displacement and potential fields:

$$u_3 = u_3(x_3) \ , \ u_1 = u_2 = 0 \ , \ \phi = \phi(x_3) \quad (25)$$

The nontrivial components of strain, electric field, stress and electric displacement are

$$S_{33} = u_{3,3} \ , \ E_3 = -\phi_{,3} \quad (26)$$

And

$$T_{11} = T_{22} = c_{13}u_{3,3} + e_{31}\phi_{,3}$$
$$T_{33} = c_{33}u_{3,3} + e_{33}\phi_{,3} \quad (27)$$
$$D_3 = e_{33}u_{3,3} - \varepsilon_{33}\phi_{,3}$$

The equation of motion and the charge equation require that

$$T_{33,3} = c_{33}u_{3,33} + e_{33}\phi_{,33} = 0$$
$$D_{3,3} = e_{33}u_{3,33} - \varepsilon_{33}\phi_{,33} = 0 \quad (28)$$

Hence

$$u_{3,33} = 0 \ , \ \phi_{,33} = 0 \quad (29)$$

Unless

$$k_{33}^2 = \frac{e_{33}^2}{\varepsilon_{33}^S c_{33}^E} = 1 \quad (30)$$

Which we do not consider because usually $k_{33}^2 < 1$. Equation (28) implies that all the strain, stress, electric field, and electric displacement components are constants.

5.2. Shorted Electrodes

Since the potential at the two electrodes are equal and E_3 is a constant, we must have

$$E_3 = 0 \quad (31)$$

The mechanical boundary conditions require that $T_{33} = p$. Then

$$S_{33} = u_{3,3} = \frac{p}{c_{33}} \ , \ T_{11} = T_{22} = \frac{c_{13}}{c_{33}}p \ , \ D_3 = \frac{e_{33}}{c_{33}}p \quad (32)$$

The work done to the plate per unit volume is

$$W_1 = \frac{1}{2}T_{33}S_{33} = \frac{p^2}{2c_{33}} \quad (33)$$

5.3. Open Electrodes

In this case the boundary conditions require that

$$T_{33} = c_{33}u_{3,3} + e_{33}\phi_{,3} = p$$
$$D_3 = e_{33}u_{3,3} - \varepsilon_{33}\phi_{,3} = 0 \quad (34)$$

Which imply that

$$S_{33} = u_{3,3} = \frac{p}{c_{33}(1+k_{33}^2)} \ , \ E_3 = -\phi_{,3} = -\frac{e_{33}}{\varepsilon_{33}c_{33}(1+k_{33}^2)}p \quad (35)$$

The work done to the plate per unit volume is

$$W_2 = \frac{1}{2}T_{33}S_{33} = \frac{p^2}{2c_{33}(1+k_{33}^2)} \quad (36)$$

5.4. Electromechanical Coupling Factor

Clearly,

$$W_1 > W_2 \quad (37)$$

The electromechanical coupling factor for the thickness-stretch of a ceramic plate poled in the thickness direction is

$$(k_{33}')^2 = \frac{W_1 - W_2}{W_1} = 1 - \frac{1}{1+k_{33}^2} = \frac{k_{33}^2}{1+k_{33}^2} \quad (38)$$

For PZT-7A, from the material constants in tables 1 and 2,

$$(k_{33}')^2 = \frac{(9.50)^2}{(235\times8.85\times10^{-12})(13.1\times10^{10})} = 0.33$$
$$k_{33}' = 0.58$$

Table 1. Mechanical properties of a few polarized ceramics [10].

Material	c_{11}	c_{12}	c_{13}	c_{33}	c_{44}	c_{66}
PZT-4	13.9	7.78	7.40	11.5	2.56	3.06
PZT-5A	12.1	7.59	7.54	11.1	2.11	2.26
PZT-6B	16.8	8.47	8.42	16.3	3.55	4.17
PZT-5H	12.6	7.91	8.39	11.7	2.30	2.35
PZT-7A	14.8	7.61	8.13	13.1	2.53	3.60
PZT-8	13.7	6.99	7.11	12.3	3.13	3.36
$BaTiO_3$	15.0	6.53	6.62	14.6	4.39	4.24
	$\times10^{10}\ N/m^2$					

Table 2. Electrical properties of a few polarized ceramics [10].

Material	e_{31}	e_{33}	e_{15}	ε_{11}	ε_{33}
PZT-4	-5.2	15.1	12.7	0.646	0.562
PZT-5A	-5.4	15.8	12.3	0.811	0.735
PZT-6B	-0.9	7.1	4.6	0.360	0.342
PZT-5H	-6.5	23.3	17.0	1.505	1.302
PZT-7A	-2.1	9.5	9.2	0.407	0.208
PZT-8	-4.0	13.2	10.4	0.797	0.514
$BaTiO_3$	-4.3	17.5	11.4	0.987	1.116
	C/m^2			$\times10^{-8}\ C/Vm$	

For other polarized ceramics, the electromechanical coupling factor k_{33}^2 are calculated and presented in Table 3.

Table 3. The electromechanical coupling factors of a few polarized ceramics.

Material	k_{33}^2
PZT-4	0.35
PZT-5A	0.31
PZT-6B	0.09
PZT-5H	0.36
PZT-7A	0.33
PZT-8	0.28
$BaTiO_3$	0.19

It is clear that PZT-5H has the most electromechanical coupling factor. Therefore, among these materials, PZT-5H is more common in comparison with other polarized ceramics.

Graphically, W_1 , W_2 and their difference are represented by areas in the Fig. 2. This figure confirms that a stiffer plate has less mechanical work, in other words, in short circuit case, the mechanical work done to the plate is more than open circuit case ($W_1 > W_2$).

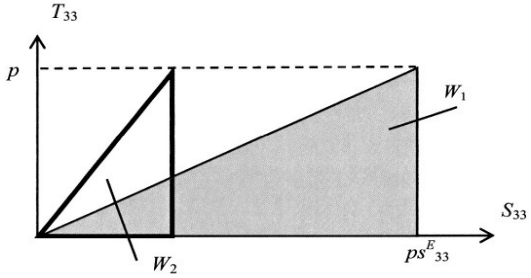

Fig. 2. Work done to the ceramic plate per unit volume along different paths [10].

6. Finite Element Method

In this section, a finite element model of the ceramic plate will be studied. The geometrical configuration of the piezoceramic plate is shown in Fig. 3.

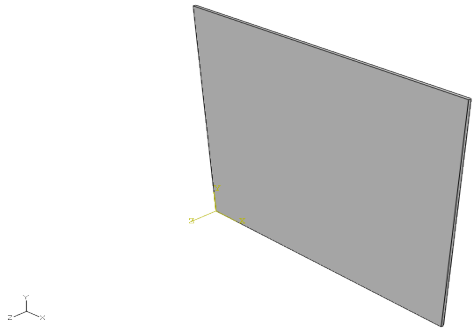

Fig. 3. The geometrical configuration of the ceramic plate.

The loaded and boundary conditions configuration of the piezoceramic plate is shown in Fig. 4.

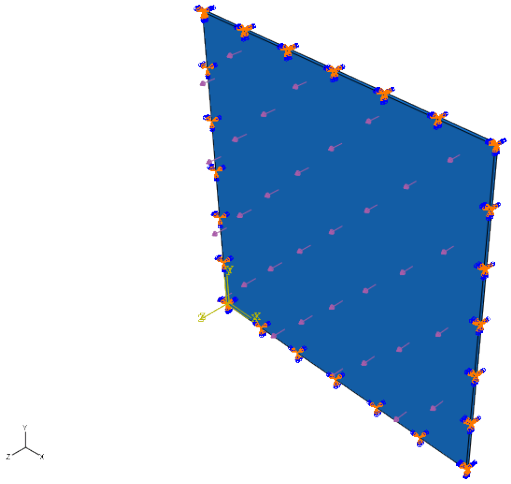

Fig. 4. The loaded and boundary conditions configuration of the ceramic plate.

The dimension of the ceramic plate is assumed to be $10cm \times 10cm \times 1mm$. The uniform normal traction is assumed to be 1 N/m^2. It will be noted that in *ABAQUS* software, the unbounded piezoelectric elements have not been defined. Therefore, the bounded piezoceramic plate is modeled, so that, the thickness ratio to other dimensions is very insignificant. Also, four edges of the plate have been modeled clamped.

A typical finite element model of the ceramic plate is shown in Fig. 5. It should be noted that ceramic plate consists of eight-node 3D linear brick piezoelectric elements (C3D8E) [12]. The finite element mesh consists of 400 elements for piezoceramic plate.

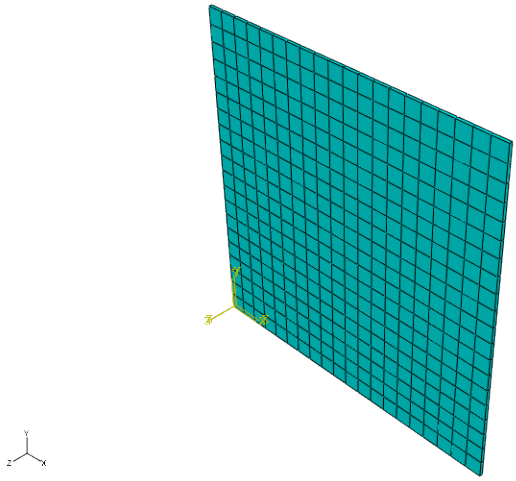

Fig. 5. Typical finite element model of the ceramic plate.

Fig. 6 shows the deformation of the piezoceramic plate under uniform normal traction obtained by finite element analysis.

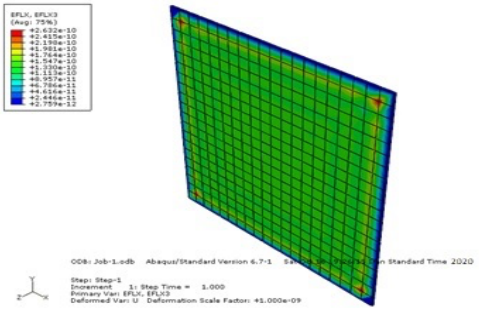

Fig. 6. Deformation of the ceramic plate by finite element analysis.

Two cases of *short circuit* (S.C) and *open circuit* (O.C) as the electrical boundary conditions were investigated and an exact solution was presented for each case. It was shown that the results obtained by the finite element analysis matches very well with the exact solutions for each boundary condition. The results obtained by the exact solution and finite element analysis for short circuit are presented in tables 4 and 5 respectively:

Table 4. The results obtained by exact solution for short circuit case.

Material	$S_{33}(m/m)$	$T_{11}=T_{22}(N/m^2)$	$D_3(C/m^2)$
PZT-4	8.70×10^{-12}	6.44×10^{-1}	1.31×10^{-10}
PZT-5A	9×10^{-12}	6.79×10^{-1}	1.42×10^{-10}
PZT-6B	6.13×10^{-12}	5.16×10^{-1}	0.44×10^{-10}
PZT-5H	8.55×10^{-12}	7.17×10^{-1}	1.99×10^{-10}
PZT-7A	7.63×10^{-12}	6.20×10^{-1}	0.72×10^{-10}
PZT-8	8.13×10^{-12}	5.78×10^{-1}	1.07×10^{-10}
$BaTiO_3$	6.85×10^{-12}	4.53×10^{-1}	1.20×10^{-10}

Table 5. The results obtained by finite element analysis for short circuit case.

Material	$S_{33}(m/m)$	$T_{11}=T_{22}(N/m^2)$	$D_3(C/m^2)$
PZT-4	8.436×10^{-12}	6.333×10^{-1}	1.33×10^{-10}
PZT-5A	8.993×10^{-12}	6.653×10^{-1}	1.482×10^{-10}
PZT-6B	5.877×10^{-12}	5.078×10^{-1}	0.424×10^{-10}
PZT-5H	8.746×10^{-12}	7.011×10^{-1}	2.114×10^{-10}
PZT-7A	7.527×10^{-12}	6.072×10^{-1}	0.736×10^{-10}
PZT-8	7.869×10^{-12}	5.673×10^{-1}	1.08×10^{-10}
$BaTiO_3$	6.420×10^{-12}	4.481×10^{-1}	1.166×10^{-10}

It is clear that in short circuit case, PZT-5A has the most strain value and PZT-5H has the most stress and electric flux density value for both exact solution and finite element method. The results obtained by the exact solution and finite element analysis for open circuit are presented in tables 6 and 7 respectively:

Table 6. The results obtained by exact solution for open circuit case.

Material	$S_{33}(m/m)$	$T_{11}=T_{22}(N/m^2)$	$E_3(V/m)$
PZT-4	6.44×10^{-12}	3.87×10^{-1}	-1.73×10^{-2}
PZT-5A	6.87×10^{-12}	4.38×10^{-1}	-1.48×10^{-2}
PZT-6B	5.62×10^{-12}	4.63×10^{-1}	-1.17×10^{-2}
PZT-5H	6.29×10^{-12}	4.55×10^{-1}	-1.12×10^{-2}
PZT-7A	5.74×10^{-12}	4.12×10^{-1}	-2.62×10^{-2}
PZT-8	6.35×10^{-12}	3.86×10^{-1}	-1.63×10^{-2}
$BaTiO_3$	5.76×10^{-12}	3.43×10^{-1}	-0.90×10^{-2}

Table 7. The results obtained by finite element analysis for open circuit case.

Material	$S_{33}(m/m)$	$T_{11}=T_{22}(N/m^2)$	$E_3(V/m)$
PZT-4	6.615×10^{-12}	3.917×10^{-1}	-1.638×10^{-2}
PZT-5A	7.293×10^{-12}	4.388×10^{-1}	-1.434×10^{-2}
PZT-6B	6.030×10^{-12}	4.564×10^{-1}	-1.123×10^{-2}
PZT-5H	6.766×10^{-12}	4.499×10^{-1}	-1.099×10^{-2}
PZT-7A	6.094×10^{-12}	4.077×10^{-1}	-2.516×10^{-2}
PZT-8	6.656×10^{-12}	3.887×10^{-1}	-1.565×10^{-2}
$BaTiO_3$	5.963×10^{-12}	3.446×10^{-1}	-0.858×10^{-2}

It is clear that in open circuit case, PZT-5A has the most strain value, PZT-6B has the most stress value and PZT-7A has the most electric field intensity value for both exact solution and finite element method.

7. Conclusions

The piezoelectric finite element capability recently made available in commercial FEA packages allows both static and dynamic analysis of fully coupled piezoelectric and structural responses. This paper reviewed the capability of the piezoelectric element provided by commercialized FEA codes, and discussed a simple case of static finite element analysis involving piezoelectric and structural coupling.

Two cases of short circuit and open circuit as the electrical boundary conditions were investigated and an exact solution was presented for each case. It was shown that the results obtained by the finite element analysis matches very well with the exact solutions for each boundary condition.

It was shown that in short circuit case, PZT-5A has the most strain value and PZT-5H has the most stress and electric flux density value for both exact solution and finite element method. Also, it was concluded that in open circuit case, PZT-5A has the most strain value, PZT-6B has the most stress value and PZT-7A has the most electric field intensity value for both exact solution and finite element method.

References

[1] Leo, D.J., " Engineering Analysis of Smart Material Systems ", Wiley, 2007.

[2] Schwartz, M., Encyclopedia of Smart Materials, John Wiley and Sons, New York, 2002.

[3] Crawley, E. F., and de Luis, J. 1987. "Use of Piezoceramic Actuators as Elements of Intelligent Structures", *AIAA J.*, Vol. 25, No.10, pp. 1373-1385.

[4] Yaman, Y., Caliskan, T., Nalbantoglu, V., Prasad, E., and Waechter, D. ICAS 2002 Congress. "Active Vibration Control of a Smart Plate", pp. 1-10.

[5] Wang, B.T., Chen, P.H., and Chen, R.L. 2006. "Finite Element Model Verification for the use of Piezoelectric Sensor in Structural Modal Analysis", *Journal of Mechanics*, Vol. 22, pp. 235-242.

[6] Benjeddou, A., Trindade, M.A., and Ohayon, R. 1997. "A Unified Beam Finite Element Model for Extension and Shear Piezoelectric Actuation Mechanisms", *Journal of Intelligent Material Systems and Structures*, Vol. 8, pp. 1012-1025.

[7] Lin, M.W., Abatan, A.O., and Rogers, C.A. 1994. "Application of Commercial Finite Element Codes for the Analysis of Induced Strain-Actuated Structures", *Journal of Intelligent Material Systems and Structures*, Vol. 5, pp. 869-875.

[8] Pouladkhan, A., Foroushani, MY., Mortazavi, A., Numerical Investigation of Poling Vector Angle on Adaptive Sandwich Plate Deflection, *International Journal of Mechanical, Industrial Science and Engineering*, vol. 8(5), pp. 795-804, 2014.

[9] Pouladkhan, A.R., Emadi, J., Habibolahiyan, H., Extension of a Smart Piezoelectric Ceramic Rod, *International Journal of Engineering and Physical Sciences*, vol. 6, pp. 157-161, 2012.

[10] Yang, J. S. 2005. "An Introduction to the Theory of Piezoelectricity", Springer.

[11] A. H. Meitzler, H. F. Tiersten, A. W. Warner, D. Berlincourt, G. A. Couqin and F. S. Welsh, III, *IEEE Standard on Piezoelectricity,* IEEE, New York, 1988.

[12] HKS, (2005) *ABAQUS User's Manual version 6.6*, (Providence, RI: Hibbitt, Karlsson, and Sorenson).

4/11/2021